Visco-Resistive MHD Modeling Benchmark of Forced Magnetic Reconnection

Matt Beidler

CEMM Meeting 10/30/2016

Acknowledging: Nate Ferraro, Chris Hegna, Jim Callen, Carl Sovinec, Brian Cornille, Andi Becerra, Torrin Bechtel, Kyle Bunkers

Motivation

- External 3D fields force magnetic reconnection (FMR), whose islands can lock in place to 3D field structure
- Suppression of edge localized modes (ELMs) by RMPs has been modeled by FMR in Callen et al., EPS (2016)
- NIMROD and M3D-C[1] codes evolve extended-MHD models that describe FMR and mode locking physics
- Benchmarking FMR with these codes is needed to understand the general linear and nonlinear responses to applied fields

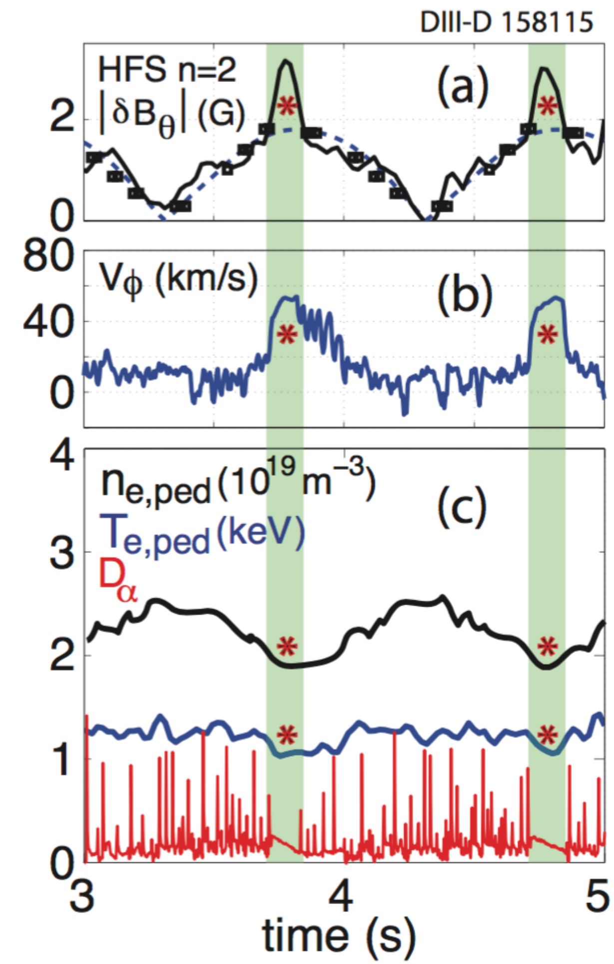

Callen et al., EPS (2016), UW-CPTC 16-3

Outline

- Description of NIMROD and M3D-C^1 codes and cylindrical benchmark parameters
- Qualitative observations of time-asymptotic FMR state
- Parametric scans of magnetic Prandtl number P_m, Lundquist number S, and axial flow
  - Comparisons to linear, time-asymptotic, analytic theory
- Nonlinear simulations of mode locking due to torque balance bifurcation in NIMROD
  - Comparisons to quasi-linear, time-asymptotic, analytic theory

NIMROD Code Is Employed to Solve the Visco-Resistive MHD Equations

- Sovinec et al., JCP (2004)
- NIMROD capable of solving extended-MHD equations
- Semi-implicit leapfrog time evolution is used:
    - Holds equilibrium fields constant and evolve perturbation fields

$$\frac{\partial \mathbf{B}}{\partial t} = -\nabla \times \mathbf{E} + \kappa_{divbd} \nabla\nabla \cdot \mathbf{B}$$

$$\mathbf{E} = -\mathbf{V} \times \mathbf{B} + \eta \mathbf{J}$$

$$\mu_0 \mathbf{J} = \nabla \times \mathbf{B}$$

$$\frac{\partial n}{\partial t} + \nabla \cdot (n\mathbf{V}) = \nabla \cdot D \nabla n$$

$$\rho \left(\frac{\partial \mathbf{V}}{\partial t} + \mathbf{V} \cdot \nabla \mathbf{V} \right) = \mathbf{J} \times \mathbf{B} - \nabla p + \nabla \cdot \rho \nu \nabla \mathbf{V}$$

$$n \frac{3}{2} \left(\frac{\partial T}{\partial t} + \mathbf{V} \cdot \nabla T \right) = -p \nabla \cdot \mathbf{V} + \nabla \cdot n \chi \nabla T$$

- Uses 2D C^0 finite elements with Fourier decomposition in 3rd dimension: $\mathbf{A}(x,y,z,t) = \mathbf{A}_0(x,y,t) + \sum_{n=1} \left[\mathbf{A_n}(x,y,t) e^{i\frac{2\pi n}{L} z} + \mathbf{A_n}^*(x,y,t) e^{-i\frac{2\pi n}{L} z} \right]$
    - (x,y,z) for slab, (r,θ,z) for cylinder with axial direction in z

M3D-C^1 Code Is Utilized to Compare with Results from NIMROD

- Ferraro and Jardin, JCP (2009)
- Semi-implicit time advance
- Uses 3D C^1 finite elements with 2D reduced quintic elements and cubic elements in the third dimension
- Evolves scalar variables f, ψ, U, ω, χ (not thermal conductivity)
  - Ensures a divergenceless magnetic field
- Formulated for (R,ϕ,Z) toroidal geometry with axial direction in ϕ
  - Adapted for cylindrical geometry

$$\frac{\partial n}{\partial t} + \nabla \cdot (n\mathbf{V}) = \nabla \cdot D \nabla n$$

$$\rho \left(\frac{\partial \mathbf{V}}{\partial t} + \mathbf{V} \cdot \nabla \mathbf{V} \right) = \mathbf{J} \times \mathbf{B} - \nabla p + \nabla \cdot \rho\nu\nabla\mathbf{V}$$

$$\mathbf{E} + \mathbf{V} \times \mathbf{B} = \eta \mathbf{J}$$

$$\frac{3}{2}\left[\frac{\partial p}{\partial t} + \nabla \cdot (p\mathbf{V})\right] = -p\nabla \cdot \mathbf{V} + \nabla \cdot n\chi\nabla T$$

$$\frac{\partial \mathbf{B}}{\partial t} = -\nabla \times \mathbf{E}, \quad \mu_0 \mathbf{J} = \nabla \times \mathbf{B}$$

$$\mathbf{A} = R^2 \nabla\phi \times \nabla f + \psi \nabla\phi - F_0 \ln R\, \hat{Z}$$

$$\mathbf{B} = \nabla\psi \times \nabla\phi - \nabla_\perp \frac{\partial f}{\partial \phi} + F\nabla\phi$$

$$F = F_0 + R^2 \nabla \cdot \nabla_\perp f$$

$$\mathbf{V} = R^2 \nabla U \times \nabla\phi + R^2 \omega \nabla\phi + \frac{1}{R^2}\nabla_\perp \chi$$

Cylindrical FMR Benchmark Between NIMROD and M3D-C[1] is Underway

- Axial current form specified according to Wesson (2004)

$$j_z(r) = j_{z0}\left[1-\left(\frac{r}{a}\right)^2\right]^\nu$$

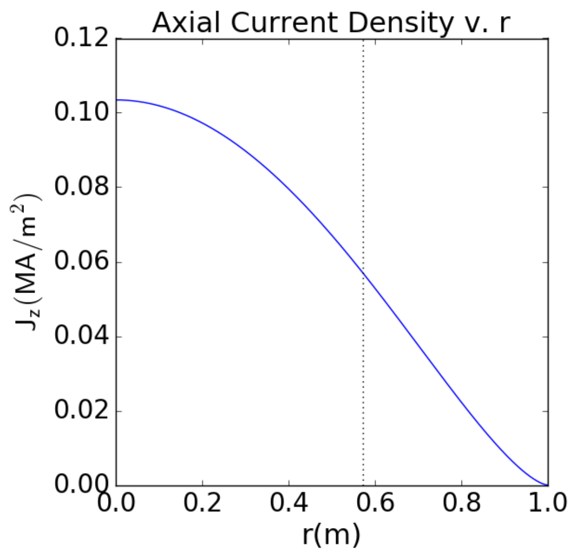

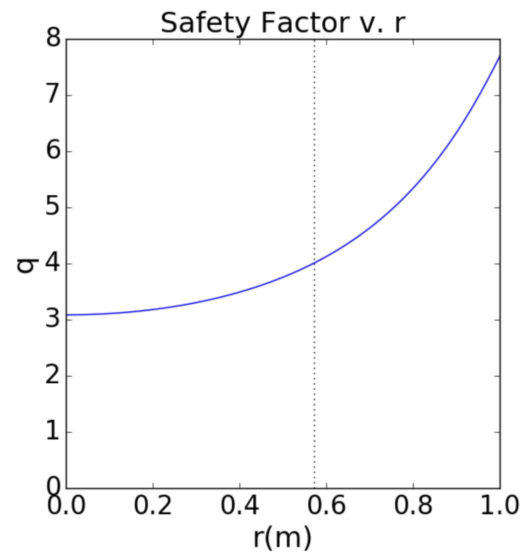

- RESTER calculates that all rational surfaces inside q=3 are resistively unstable

- $j_{z0} = 0.103$ MA/m^2, $\nu = 1.50$, $B_{z0} = 1$T, $R_0 = 5$m
  - ➢ q(r=0)=3.08, q(r=a)=7.68, r(q=4) $\equiv$ r_s=0.572m

- RESTER calculates $\boxed{r_s\Delta'_{q=4} = -2.52}$

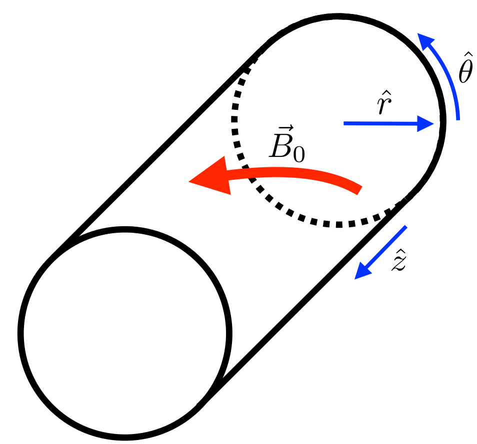

Physical Parameters Are Chosen for Cylindrical Benchmark

- Constant β = 8x10^{-4}, constant n = 10^{19} m^{-3}, isotropic χ = 2 m^2/s
- Vary resistivity around η = 2.51x10^{-6} Ω·m to vary Lundquist number
  - S_G based on background axial field $S_G = a\frac{B_{z0}}{\eta}\sqrt{\frac{\mu_0}{\rho}} = 3.45\times10^6$
  - S_L based on reconnecting field $S_L = \frac{nsr_s^2}{R_0}\frac{B_{z0}}{\eta}\sqrt{\frac{\mu_0}{\rho}} = 1.27\times10^5$, with $s = \frac{r}{q}\frac{dq}{dr}\Big|_{r_s}$ and axial mode n
- Vary viscosity around μ = 2x10^{19} kg/(m·s) to vary magnetic Prandtl number around P_m = 1
  - $\delta_{VR} = S_L^{-1/3}P_m^{1/6}r_s = 3.60\times10^{-3}$ m
- Edge resistivity and viscosity profiles ~$[1+(\Delta_{vac}^{1/2}-1)*(r/a)^{\Delta_{exp}}]^2$
  - Δ_{vac} =1000 increasing diffusivity, Δ_{exp} =25 for thin edge region

Equilibrium Perturbed at Lowest Order q=4 Rational Surface

- Normal magnetic field set at r=a: $B_{r,1}(r=a,\theta,z)=B_{nw}\, e^{i[m\theta+(n/R_0)z]}$
- Normal field evolution of $B_{r,1}(\mathbf{r},t)=B_r(\mathbf{r})[1-e^{-t/\tau_{nw}}]$
  - M3D-C[1] solves time-independent system
- FMR at q=4 surface with (m,n)=(-4,1) perturbation
  - Helicity of (m,n)=(-2,2) in left figure
  - Comparison of vacuum fields in right figures

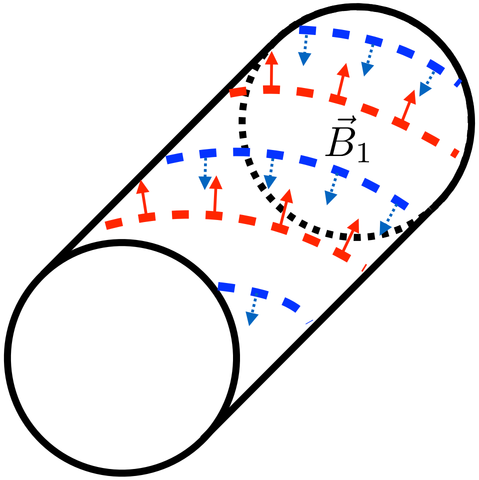

NIMROD

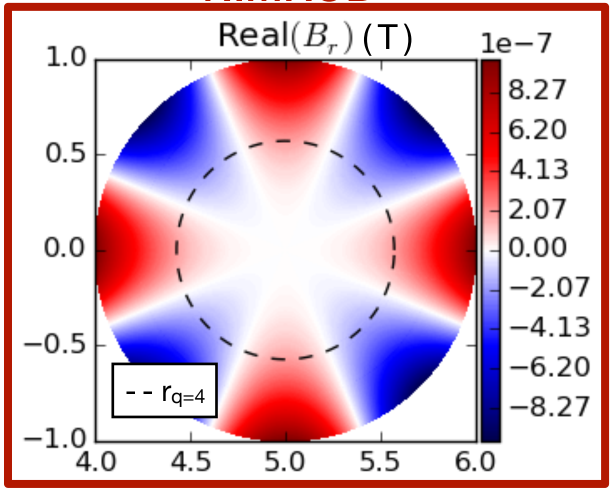

M3D-C[1]

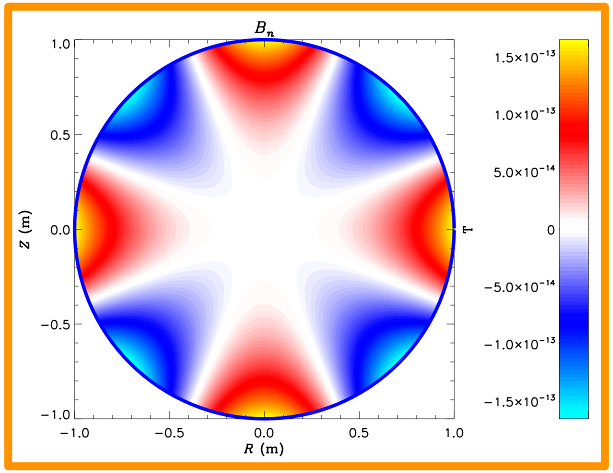

Evolution of Cylindrical FMR in NIMROD is Qualitatively Consistent with Analytic Predictions

- Asymptotic field response at $r=r_s$ is $B_{r,obs}(r_s) = 2.17\times10^{-7}$ T , which differs from predicted value of $B_{r,pre}(r_s) = 2.05\times10^{-7}$ T
- Overshoot occurs on visco-resistive tearing timescale $\tau_T \sim \tau_H S_L^{2/3} P_m^{1/6} = 1.4\times10^{-3}$ s
    - Alfvén time based off reconnecting field

$$\tau_H = \frac{R_0}{B_{z0}} \frac{\sqrt{\mu_0 \rho}}{ns}$$

- Asymptotic B_r response at $r \lesssim r_s$ is increased over vacuum, decreased at $r \gtrsim r_s$

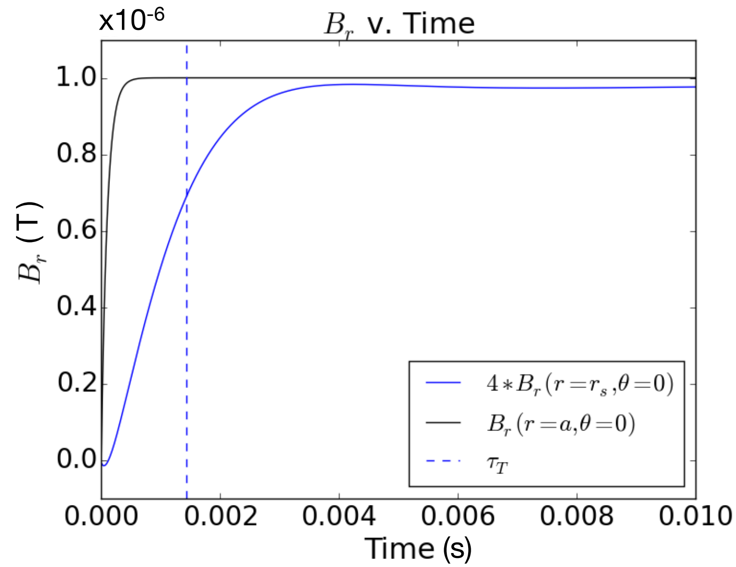

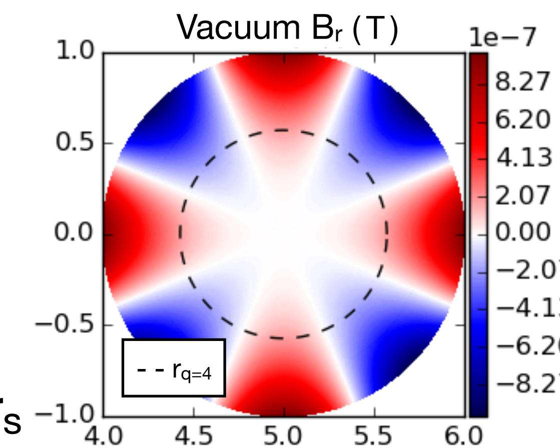

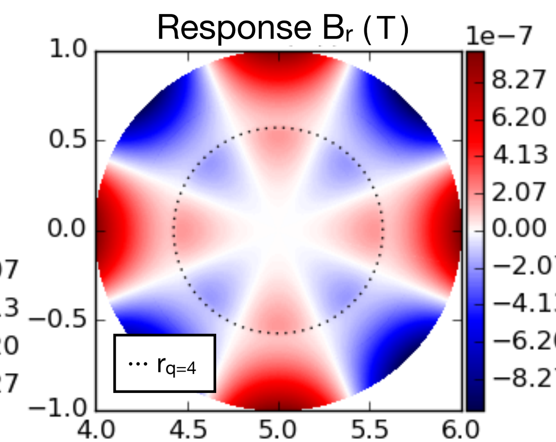

Flow Patterns Localized Around Rational Surface Occur in Time-Asymptotic State

- Time-asymptotic flow patterns *do not occur in slab geometry*
- Flow pattern shown for P_m=1
  - Radial flows are even across r_s and poloidal flows are odd across r_s
  - Opposite of tearing parity
- Width of vortices scale similarly as δ_{VR}

NIMROD

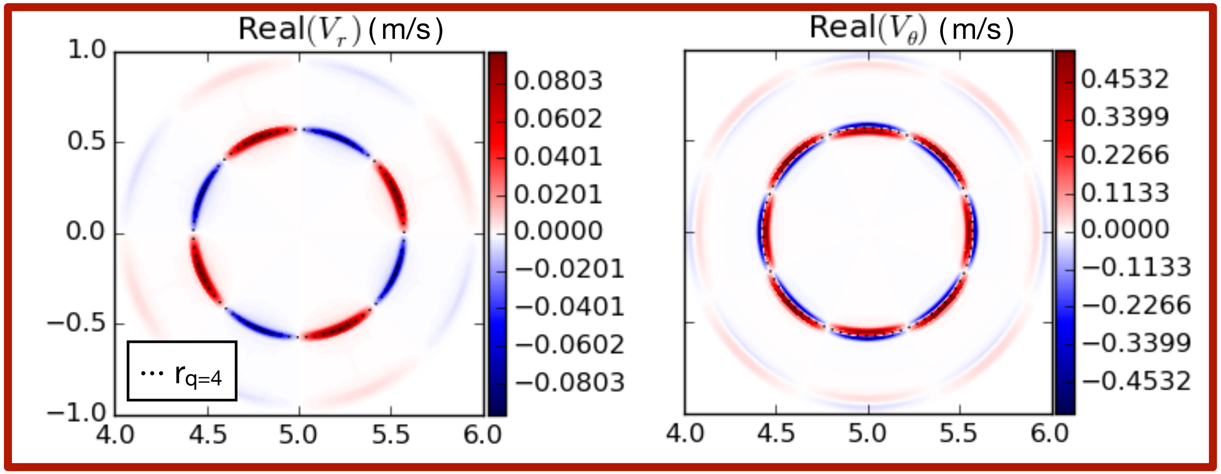

M3D-C[1]

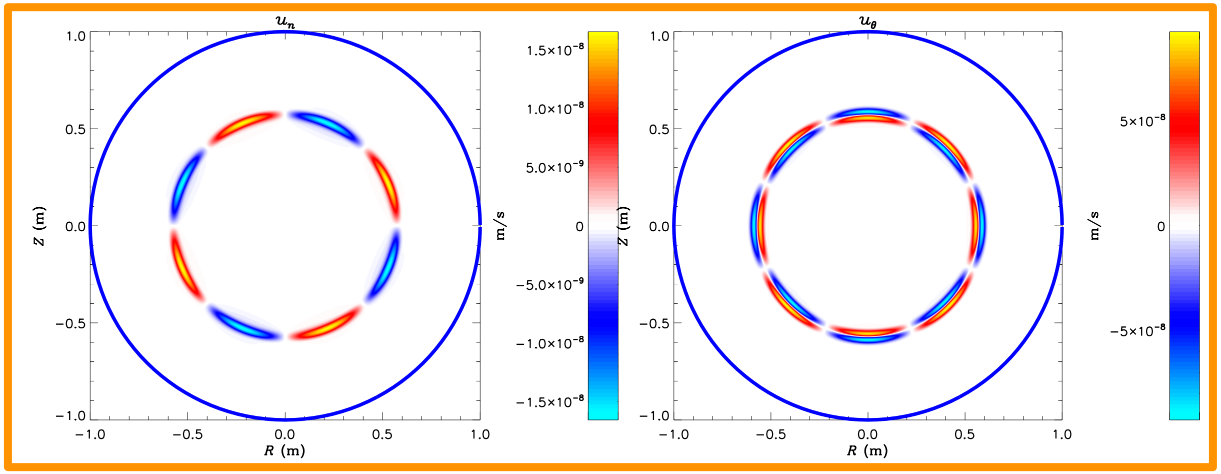

Field Response Scales with Magnetic Prandtl Number P_m

- Fitzpatrick theory has no dependence on P_m for zero flow
  - Physical effect of localize 3D visco-resistive equilibrium?
- Excellent agreement between codes for experimentally relevant P_m ~1
  - Slight disagreement at lowest P_m

NIMROD

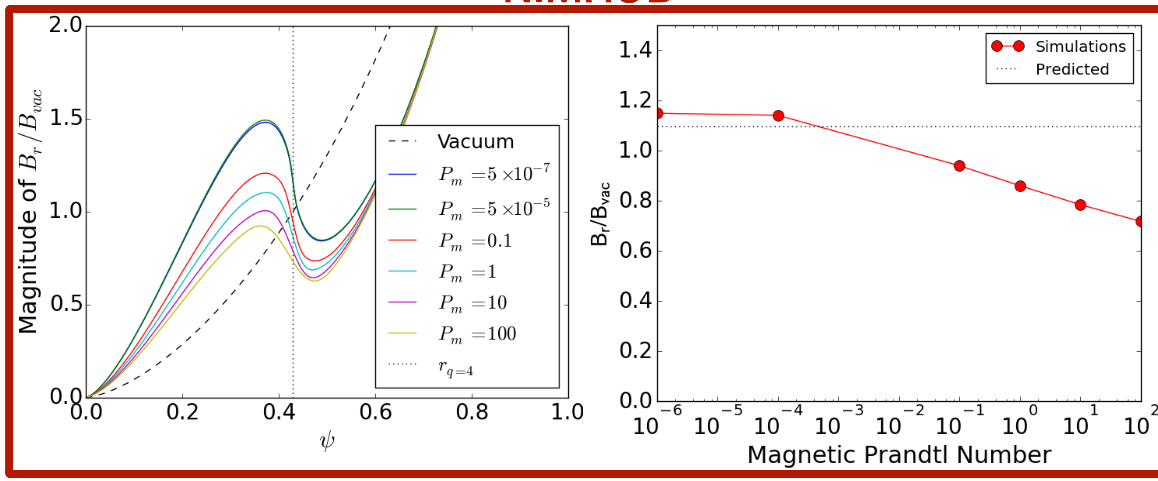

M3D-C[1]

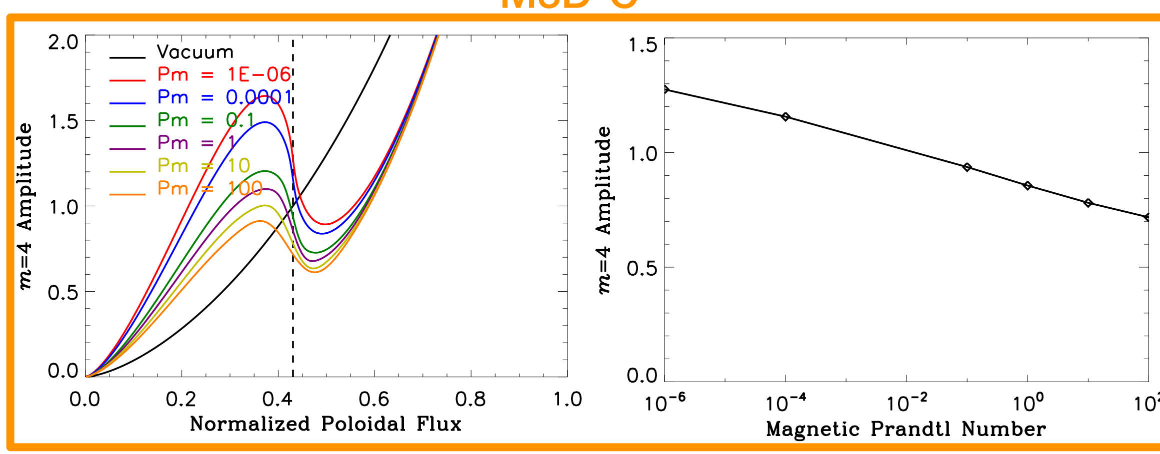

Field Response Scales with Lundquist Number S_G

- Fitzpatrick theory has no dependence on S_G for zero flow
  - Physical effect of localized 3D visco-resistive equilibrium?
- Excellent agreement between codes for all tested S_G

NIMROD

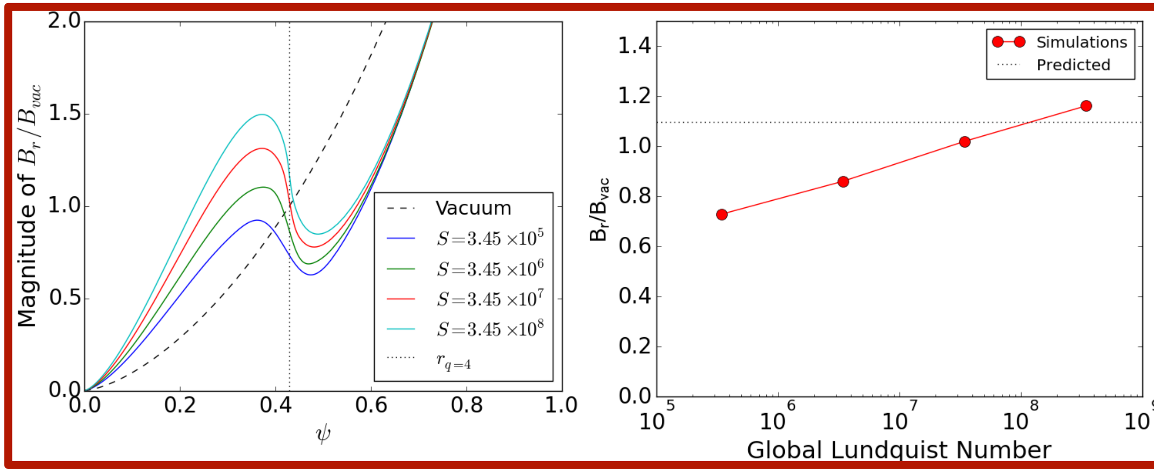

M3D-C[1]

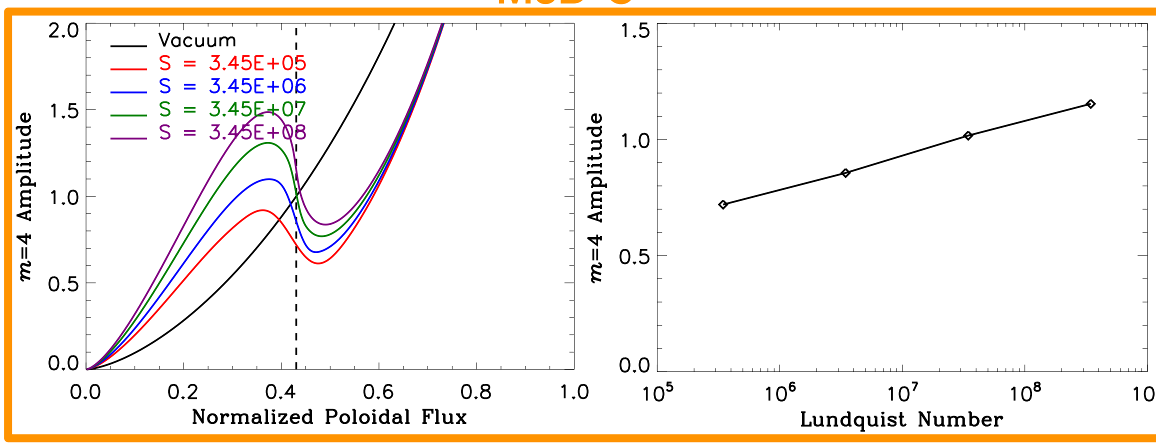

NIMROD Shows Flow-Screening with Inclusion of Axial Flow

- Flow at r_s causes changing magnetic perturbation in reference frame of moving plasma
  - Generates eddy currents that 'screen out' applied fields

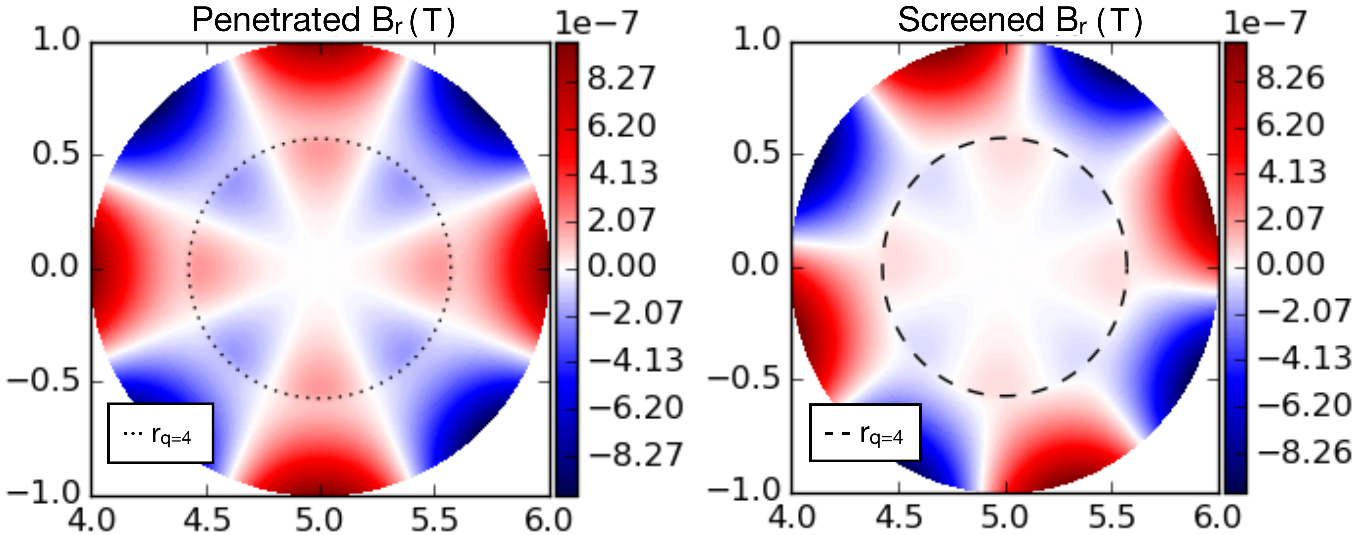

- $\omega = \vec{k} \cdot \vec{v}$ quantifies convection in space or modulation in time
  - Right figure has $\omega = 2$ krad/s (v_z=10 km/s) and is shown at t=0.01s
- 'Phase' refers to relative poloidal alignment between magnetic response at r_s and perturbation at boundary
  - 0°: (max/min) edge color with same r_s color; 90°: edge color with no r_s color; 180°: edge color with opposite r_s color

NIMROD and M3D-C[1] Simulations Exhibit Similar Flow-Screened Mode Structure

- Excellent agreement between codes for all tested v_z
  - Slight difference in phase due to approximate measurement of m=4 mode used in NIMROD
- Alfvén resonances appear when phase > 90°

NIMROD

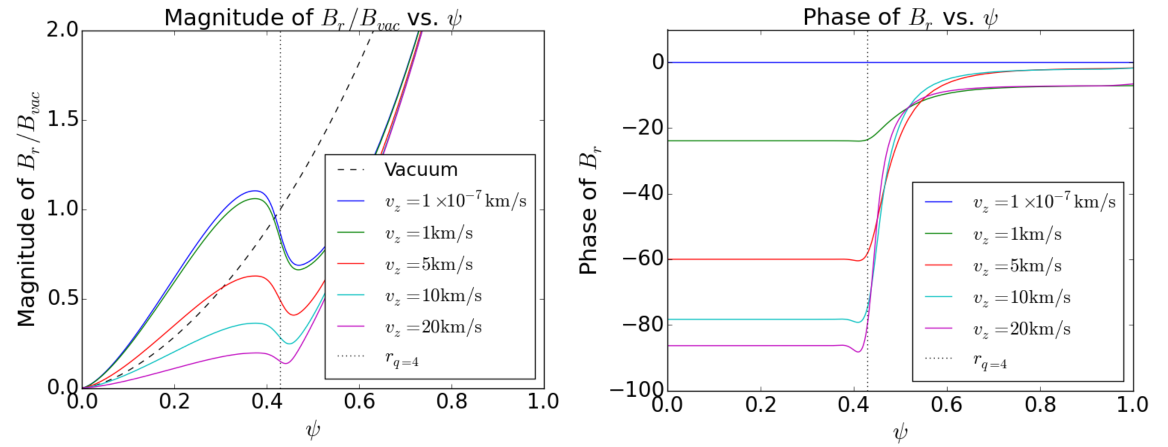

M3D-C[1]

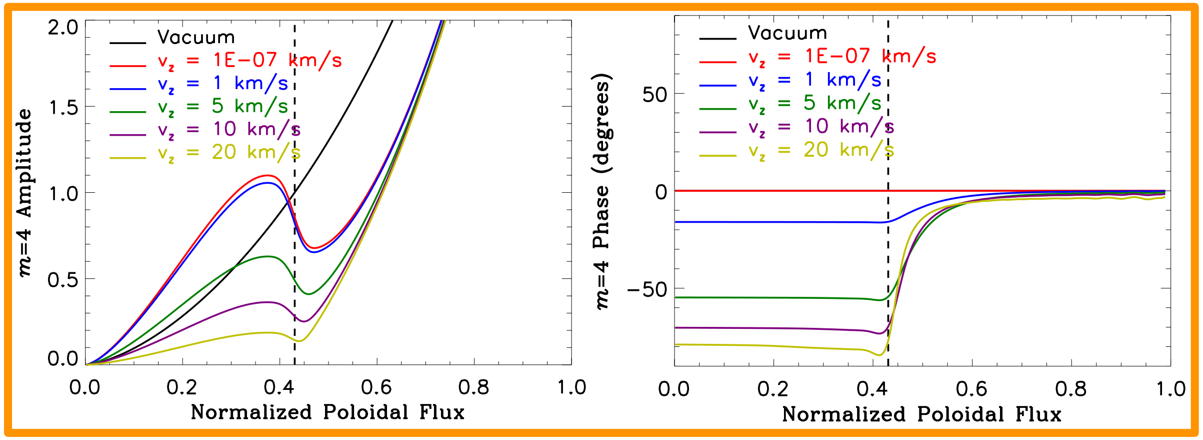

Linear Field Response Is Flow-Screened According to Time-Asymptotic Fitzpatrick Theory

- Assume total flux function is composed of forced-tearing plasma response and shielded components: $\psi_{\rm tot} = \psi_T + \psi_S$ for $\mathbf{B} = \hat{\mathbf{z}} \times \nabla\psi$
  - Boundary conditions on shielded solution: $\boxed{\psi_S(r \le r_s) = 0,\ \psi_S(r=a) = \psi(a)}$
  - Boundary conditions on tearing solution: $[\![\psi_T]\!]_{r_s} = 0$, $\psi_T(r=a) = 0$
- Jump condition in radial derivative of total flux function across rational surface with instability and flow according to Fitzpatrick, POP (1994) gives:

  $r_s[\![\partial_r\psi_{tot}]\!]_{r_s} = r_s[\![\partial_r\psi_T]\!]_{r_s} + r_s[\![\partial_r\psi_S]\!]_{r_s}$

  ➛ $i\omega\tau_S\psi(r_s) = \psi(r_s) r_s\Delta' + \psi(a) r_s\Delta'_{ext}$
  - $\tau_S = 2.104\, \tau_H\, S_L^{2/3} P_m^{1/6}$ for VR regime

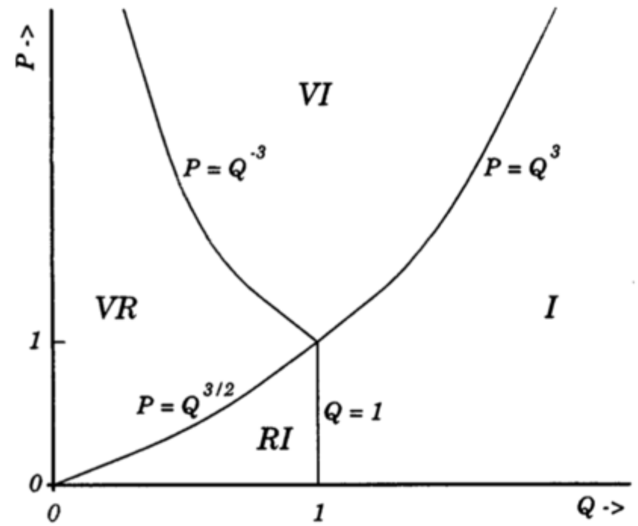

- RESTER evaluation of $r_s[\![\partial_r\psi_S]\!]_{r_s} \equiv \psi(a) r_s\Delta'_{ext}$ gives $r_s\Delta'_{ext} = 0.518$
- Field response is given by $\boxed{B_r(r_s) = \dfrac{r_s\Delta'_{ext}}{-r_s\Delta' + i\omega\tau_s} B_{nw}}$

Simulations of Flow-Screening Are Qualitatively Consistent with Fitzpatrick Predictions

- Excellent agreement between codes for all tested v_z
- Difference from analytics a physical effect of localized 3D visco-resistive equilibrium?
- Alfvén resonances appear for $v_{\phi,0} > 20$ km/s

NIMROD

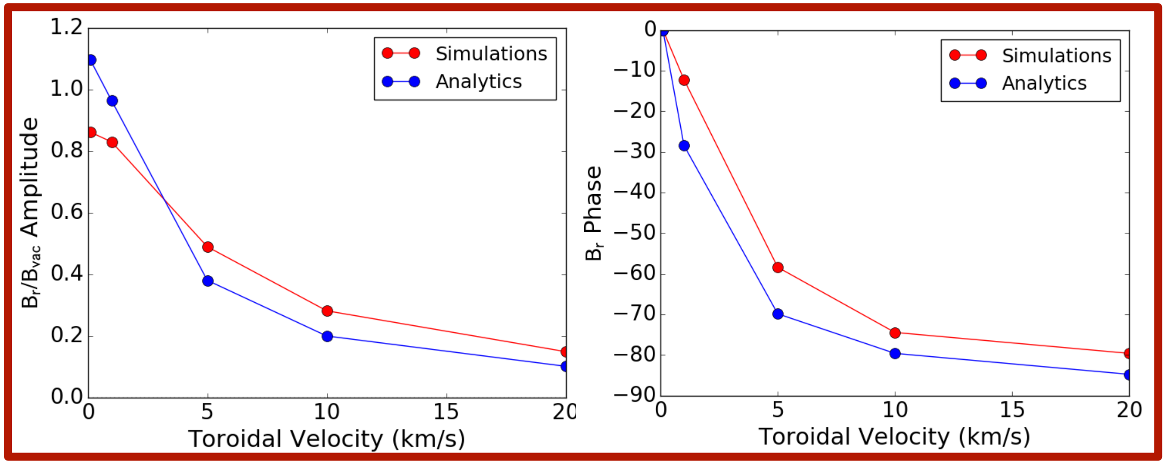

M3D-C[1]

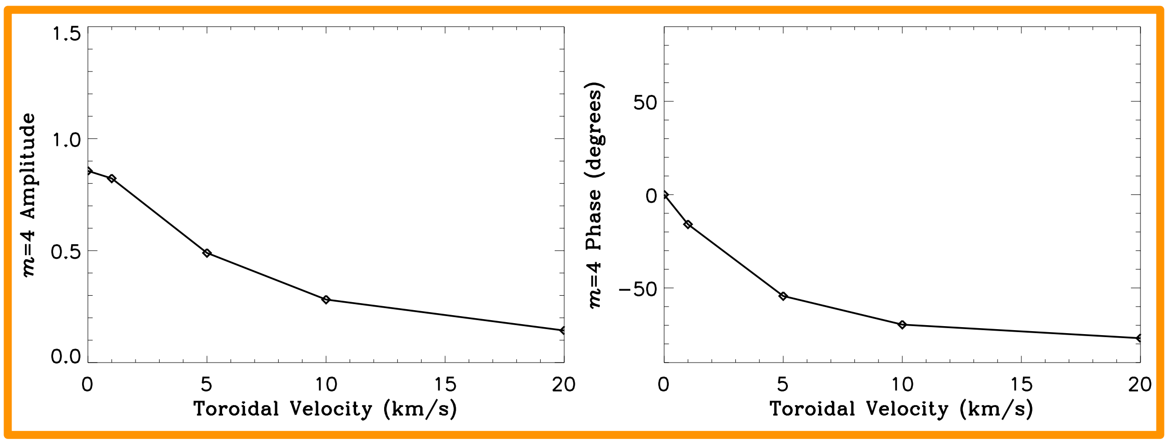

Flow-Screened Response Scales with Magnetic Prandtl and Lundquist Numbers in NIMROD

- P_m scans done at S_G=3.45x10^6 and Q=0.389 ($\omega = 2$ krad/s)
  - Simulations span VI (P>Q^{-3}), VR (Q$^{2/3}$<P<Q^{-3}), RI (P<Q$^{3/2}$) regimes
- S_G scans done at P_m=1 and Q=0.389
  - Simulations span VR (Q<1) and inertial (Q>1), where Alfvén resonances appear

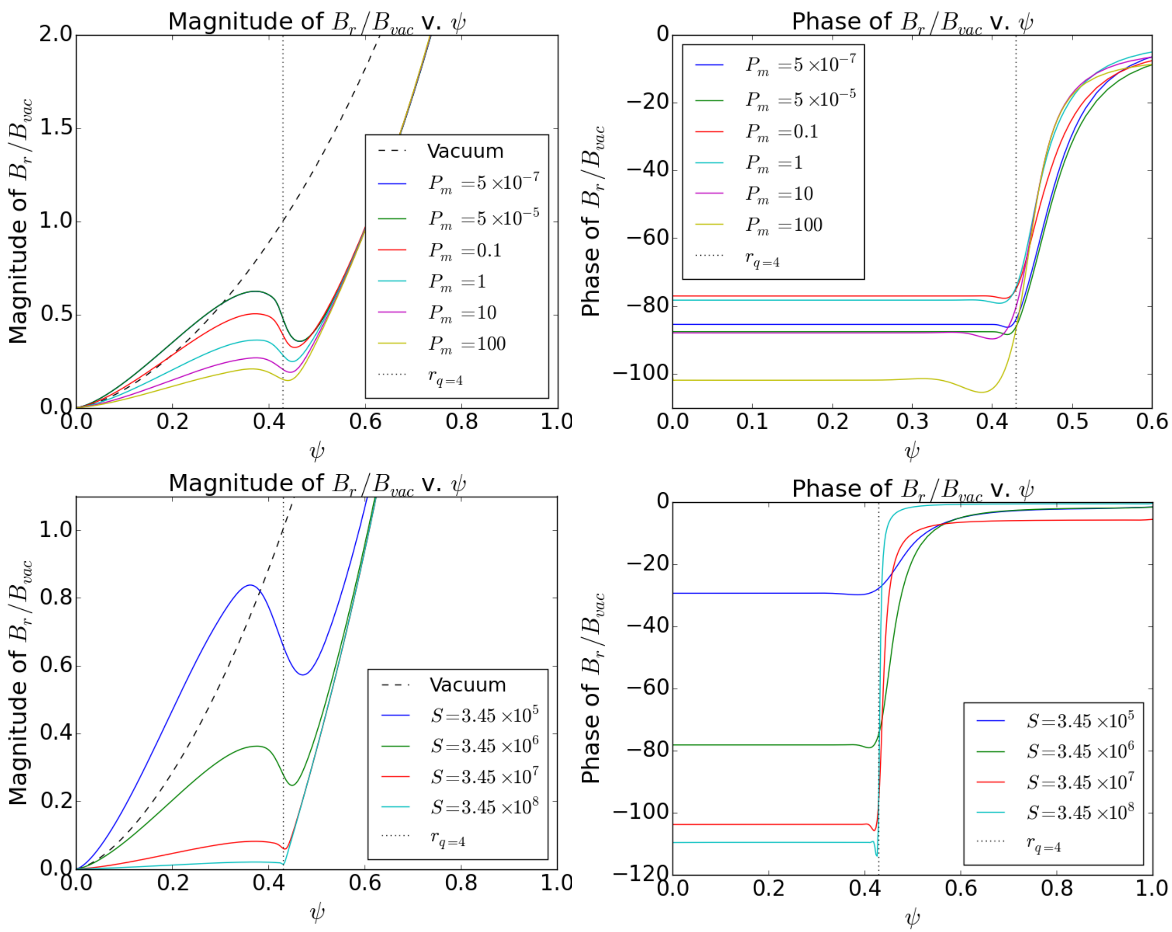

Nonlinear Electromagnetic and Viscous Force Balance Gives Rise to Mode Locking Bifurcation

- Integrating θ, z components of **J**×**B** and $\nabla\cdot\rho\nu\nabla\mathbf{v}$ over θ, z and radially about r_s gives time-asymptotic n = 0 electromagnetic and viscous torques [Fitzpatrick, NF (1993)]

$$\delta T_{EM,\theta} = \frac{-8\pi^2 R_0 r_s^2}{\mu_0 m} \frac{(r_s\Delta'_{ext})^2\omega\tau_s}{(-r_s\Delta')^2 + (\omega\tau_s)^2} B_{nw}^2 \qquad \delta T_{EM,z} = \frac{n}{m}\delta T_{EM,\theta}$$

$$\delta T_{VS,\theta} = -4\pi^2 R_0 r_s^2 \mu(r_s) \left[1 + \frac{1}{\mu(r_s)\int_{r_s}^{a}\frac{dr'}{r'\mu(r')}}\right]\Delta\Omega_\theta(r_s) \equiv \mu_\theta \Delta\Omega_\theta(r_s) \quad \delta T_{VS,z} = \frac{-4\pi^2 R_0^3}{\int_{r_s}^{a}\frac{dr'}{r'\mu(r')}}\Delta\Omega_z(r_s) \equiv \mu_z\Delta\Omega_z(r_s)$$

  - Where $\omega - \omega_0 = m\Delta\Omega_\theta(r_s) + n\Delta\Omega_z(r_s)$ is the flow response at r_s

- Force balance in θ, z gives cubic relation in ω

$$\boxed{\frac{\omega_0}{\omega} - 1 + \omega_0\omega\tau_s^{*2} - \omega^2\tau_s^{*2} = \frac{-8\pi^2 R_0 r_s^2 \tau_s}{\mu_0 m^2}\left(\frac{\Delta'_{ext}}{\Delta'}\right)^2 B_{nw}^2 \left[\frac{m^2}{\mu_\theta} + \frac{n^2}{\mu_z}\right]}$$

where $\tau_s = 2.104\tau_H S_L^{2/3} P_m^{1/6}$ for VR regime and $\tau_s^* = \frac{\tau_s}{-r_s\Delta'}$

- Bifurcation when initial angular frequency exceeds $\boxed{\omega_{0,crit} = \frac{3\sqrt{3}}{\tau_s^*}}$

WISCONSIN
UNIVERSITY OF WISCONSIN–MADISON

Nonlinear Mode Locking in Cylindrical Simulations is Quantitatively Consistent With Analytics

- Field screening caused by inductively driven eddy currents
  - Plasma stationary with modulated applied field
    - $B_{r,1}(\mathbf{r},t)=B_r(\mathbf{r})[1-e^{-t/\tau_{nw}}]e^{i(2\pi f)t}$
    - Red data of modulated field at $f=0.318$ kHz $> f_{crit}=0.305$ kHz
  - Plasma flowing (with flat-top velocity profile) through static applied field
    - $B_{r,1}(\mathbf{r},t)=B_r(\mathbf{r})[1-e^{-t/\tau_{nw}}]$
    - Blue data has plasma flowing with $\omega_0=2$ krad $> \omega_{crit}=1.91$ krad
- Excellent agreement between simulation and analytic predictions for both cases

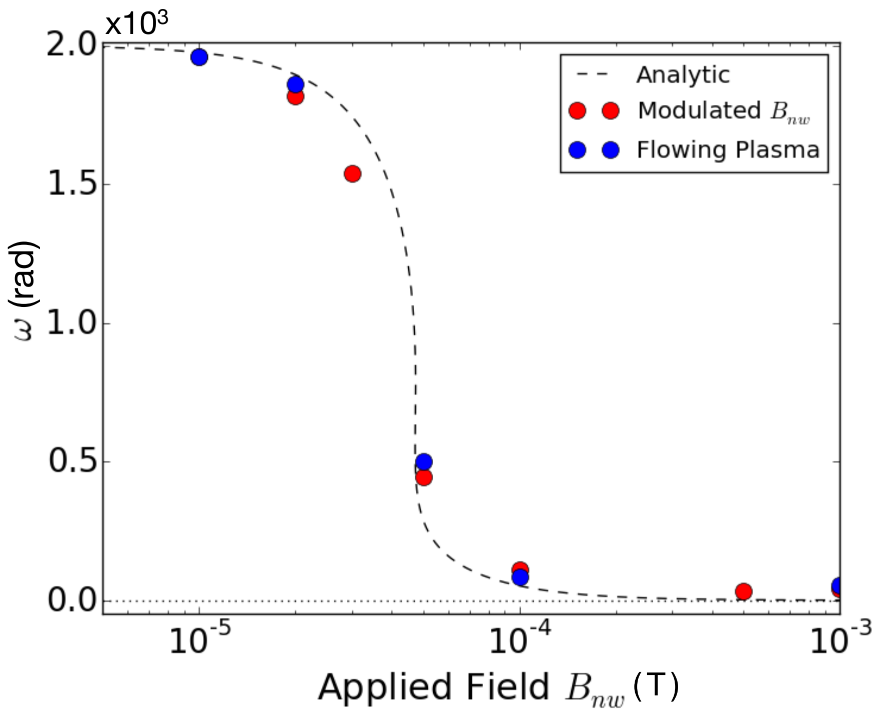

Poloidal Flow Response Dominates Axial Flow Response in Mode Locking

- Flow response is localized to the rational surface
- Poloidal flow response dominates due to smaller moment arm for poloidal viscous torque
  - Viscous damping smaller by square of aspect ratio
  - μ_θ=-7.82x10^{-6}, μ_z=-4.32x10^{-4}
- v_z for $r<r_s$ is relaxing toward flat profile in time-asymptotic state

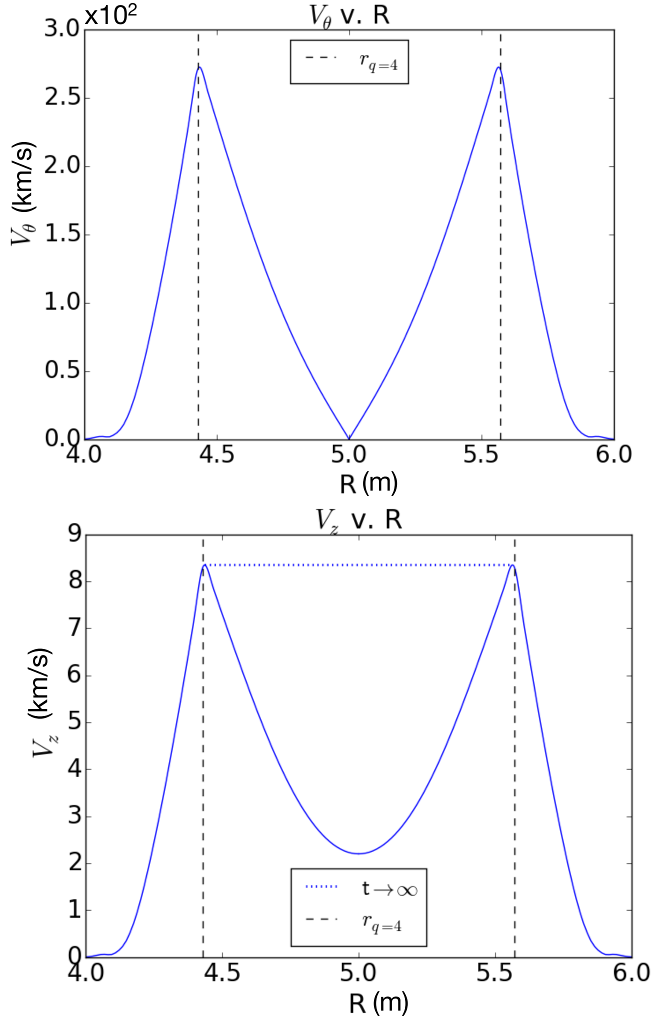

Ongoing and Future Work

- Nonlinear benchmarking with NIMROD and M3D-C^1
- Investigate the role that the localized 3D visco-resistive equilibrium plays in field response in cylindrical geometry
- Explore various physics questions in the cylindrical geometry
  - Transient MHD events triggering mode locking
  - Nonlinear coupling in field response
- Begin to model RMPs in toroidal geometry
  - Circular cross section test equilibrium
  - Well diagnosed DIII-D experimental cases

Conclusions

- Cylindrical benchmark with NIMROD and M3D-C^1 is underway, and linear comparison of penetrated magnetic field response to flow screening shows excellent agreement
  - Observation of localized 3D visco-resistive equilibrium
- Nonlinear simulations in cylindrical geometry quantitatively agree with analytics of mode locking bifurcation
  - Poloidal torque effects dominate mode locking flow response